Journal Pre-proof

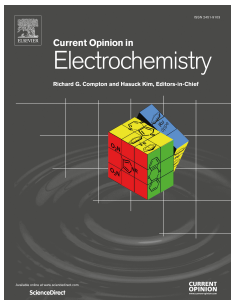

Stepwise Electrochemical Layer-by-Layer Characterisation for the Controlled Assembly of Multilayered (Bio)sensors

R. Cancelliere, PhD, Research Scientist, A. Licheri, PhD, student, E. Paialunga, PhD, L. Micheli, PhD, Associate Professor

PII: S2451-9103(26)00066-9

DOI: https://doi.org/10.1016/j.coelec.2026.101875

Reference: COELEC 101875

To appear in: *Current Opinion in Electrochemistry*

Received Date: 26 March 2026

Revised Date: 11 May 2026

Accepted Date: 16 May 2026

Please cite this article as: Cancelliere R, Licheri A, Paialunga E, Micheli L, Stepwise Electrochemical Layer-by-Layer Characterisation for the Controlled Assembly of Multilayered (Bio)sensors, *Current Opinion in Electrochemistry*, https://doi.org/10.1016/j.coelec.2026.101875.

Information to appear on the first page of your article

Title: Stepwise Electrochemical Layer-by-Layer Characterisation for the Controlled Assembly of Multilayered (Bio)sensors

Authors:

Rocco Cancelliere, PhD, Research Scientist, *ENEA, Technologies and Devices for Electrochemical Storage (TERIN-DEC-ACEL), Rome 00123, Italy*

Antonio Licheri, PhD student, *Department of Chemical Science and Technologies, University of Rome Tor Vergata, Rome 00133, Italy*

Elisa Paialunga, PhD, *Department of Chemical Science and Technologies, University of Rome Tor Vergata, Rome 00133 Italy* and *SANA S.r.l., Corso Lazio 17 (Scala B), 03100, Frosinone, Italy*

Laura Micheli, PhD, AssociatePprofessor, Department of Chemical Science and Technologies, University of Rome Tor Vergata, Rome 00133 Italy

Conflict of Interests:

Updated November 2021

☒ The authors declare that they have no known competing financial interests or personal relationships that could have appeared to influence the work reported in this paper.

☐ The authors declare the following financial interests/personal relationships which may be considered as potential competing interests:

Corresponding author address (Street and full postal address, without the institution or department):

Correspondence telephone (please follow format +1 XXX XXX XXXX for US Nos):

Correspondence email:

<u>Information to appear on the end pages of your article before the references</u>

Acknowledgment and funding sources:*

***(Please note that you should not include a statement to the effect that there is no acknowledgment or funding, only actual funding details or acknowlegments should be included in this section)**

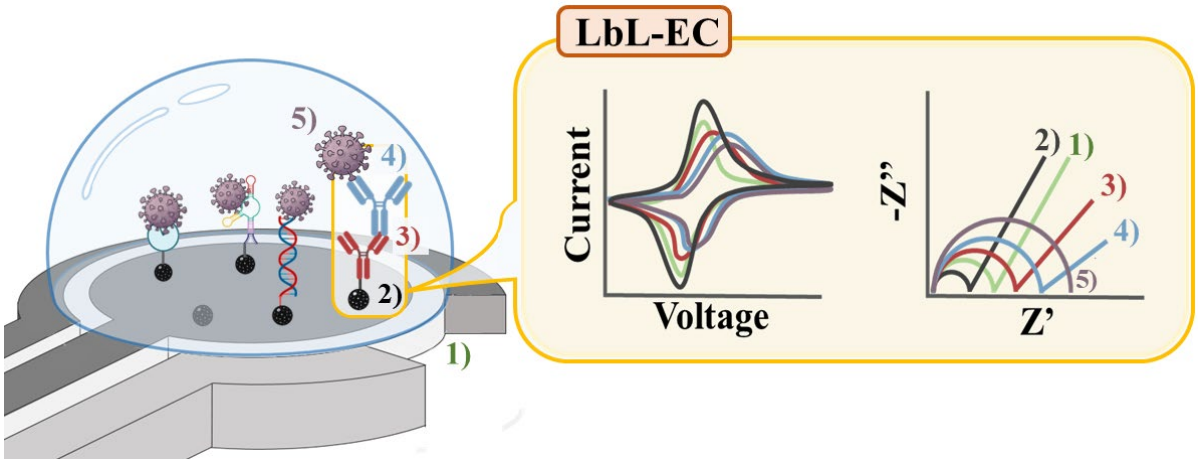

Graphical Abstract

Stepwise Electrochemical Layer-by-Layer Characterisation for the Controlled Assembly of Multilayered (Bio)sensors

R. Cancelliere[1,Ω,*], A. Licheri[2,Ω], E. Paialunga[2,3], L. Micheli[2,*]

[1]*ENEA, Technologies and Devices for Electrochemical Storage (TERIN-DEC-ACEL), Rome 00123, Italy*
[2] *Department of Chemical Science and Technologies, University of Rome Tor Vergata, Roma*
[3]*SANA S.r.l., Corso Lazio 17 (Scala B), 03100, Frosinone, Italy*
[Ω] *These two authors contributed equally*
[*]*Corresponding Authors: rocco.cancelliere@enea.it, laura.micheli@uniroma2.it.*

Abstract:

Electrochemical layer-by-layer characterisation (LbL-EC) is emerging as a powerful strategy for the controlled fabrication of multilayered electrochemical (bio)sensors. By enabling stepwise electrochemical monitoring of assembly processes, LbL-EC provides access to key interfacial parameters, including film growth, composition, and bioreceptor integration, thereby supporting the optimisation of assembly conditions and the reproducible fabrication of sensing interfaces. This control can lead to improved sensitivity, stability, and durability by regulating interfacial charge transfer and surface coverage.

Techniques such as cyclic voltammetry and electrochemical impedance spectroscopy, applied individually or synergistically, offer probe-dependent insights into interfacial charge transport, surface coverage, and electron-transfer kinetics. In this context, electrochemical responses reflect not only intrinsic interfacial properties but also their interaction with the selected redox probe.

This review discusses the fundamental mechanisms governing mass and charge transport within multilayer architectures and critically evaluates the strengths and limitations of LbL-EC as a monitoring and interpretative tool. A comparative analysis with conventional imaging methods, including transmission electron microscopy, scanning electron microscopy, atomic force microscopy, and scanning tunnelling microscopy, highlights the complementary roles of structural and electrochemical characterisation.

Overall, LbL-EC provides a framework for linking electrochemical parameters with interfacial properties, supporting the rational optimisation and reproducible fabrication of multilayer (bio)sensing interfaces.

Keywords: electrochemical layer-by-layer assembly characterisation, layer-by-layer assembly, stepwise electrode modification, electron transfer mechanisms, bioreceptor immobilisation, (Bio)sensing technologies.

Graphical Abstract

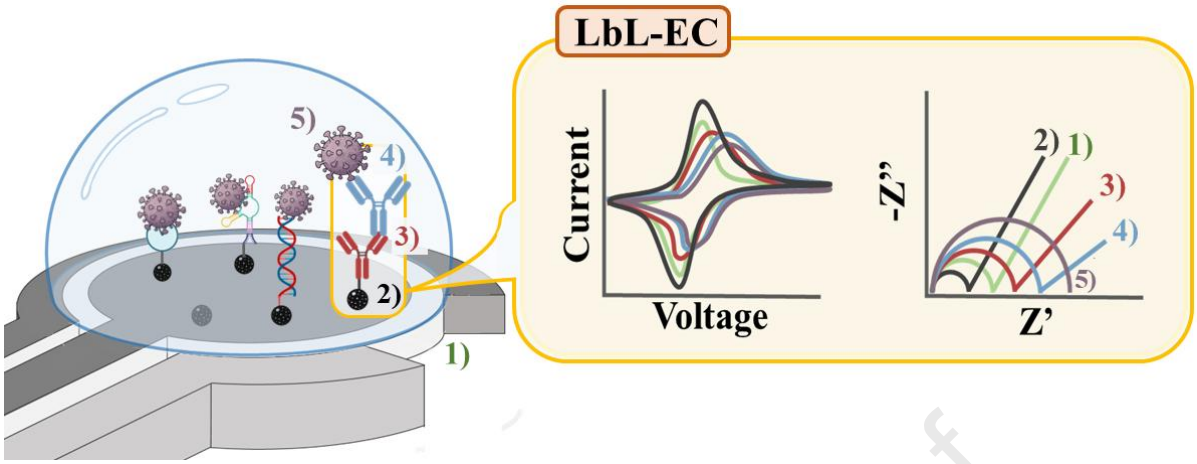

1. Introduction

Electrochemical biosensors (EBs) have become indispensable tools in healthcare diagnostics, environmental monitoring, and industrial safety, owing to their ability to rapidly, sensitively, and selectively detect a wide range of targets using biological or synthetic bio-recognition elements [1–3].

Within this landscape, the layer-by-layer (LbL) assembly technique has introduced a paradigm shift by enabling tailored interfaces with precise control over composition, thickness, and morphology [4]. In its classical definition, LbL refers to polyelectrolyte multilayer assembly via repeated adsorption cycles. Here, we use the term in a broader sense to denote the stepwise construction of biosensor interfaces through the sequential deposition of nanomaterials, bioreceptors, and blocking layers. Such structural tuning maximises analyte–surface interactions, minimises nonspecific interference, and ultimately enhances signal output and sensor reliability [5,6]. Yet, the increasingly complex architectures of multilayered biosensors, comprising nanomaterials, blocking agents, and biorecognition elements, demand advanced characterisation methods capable of probing each layer with high resolution to ensure correct assembly and functionality [7–12](see Figure 1).

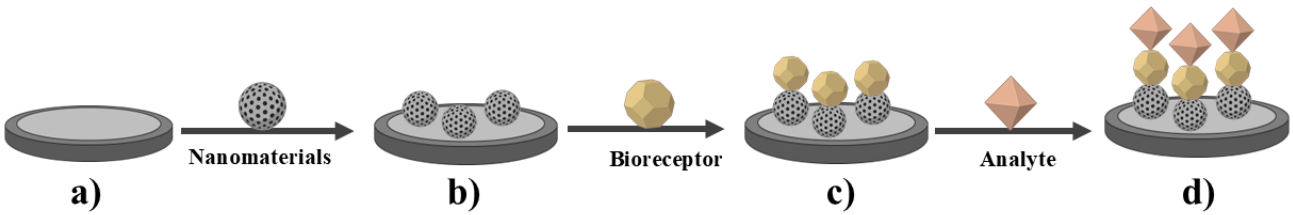

Figure 1: Schematic representation of a LbL assembly-based biosensor architecture. a) Bare electrochemical transducer, exemplified by a screen-printed electrode (SPE), b) modification of the

working electrode (WE) surface with a nanomaterial, c) immobilisation of a bioreceptor and d) detection of the target analyte.

Among these, electrochemical layer-by-layer characterisation (LbL-EC) has emerged as a rapid, cost-effective, and uniquely powerful approach, enabling *in situ* and real-time monitoring of layer deposition and interfacial behaviour [13]. Unlike conventional imaging techniques such as scanning or transmission electron microscopy (SEM, TEM) and atomic force microscopy (AFM), which provide static snapshots, LbL-EC captures the dynamic interactions between multilayers and their surrounding environment [14,15].

This review critically examines LbL-EC as a strategy for advancing biosensor design. Its capabilities were compared with those of other characterisation techniques, elucidating the fundamental insights it provides into mass and charge transport, and highlighting its role in guiding rational decision-making through sensor assembly. Emphasis is placed on cyclic voltammetry (CV) and electrochemical impedance spectroscopy (EIS) as key tools for layer investigation. Finally, both successful and less effective applications were discussed, providing practical perspectives on how LbL-EC can accelerate the development of next-generation biosensors.

2. Advantages and Limitations of LbL-EC: A Comparative Assessment of Characterisation Methods

Surface analysis techniques provide crucial insights into the morphology and organisation of multilayered (Bio)sensor architectures. Conventional surface analysis techniques remain indispensable for resolving morphology at different scales. SEM enables assessment of overall film uniformity, TEM reveals nanostructured domains, while AFM and Scanning Tunnelling Microscopy (STM) probe topography and molecular packing density with near-atomic resolution [16–21]. Yet, these methods remain fundamentally static: they typically require high vacuum environments, which can induce artefacts such as cracking or dehydration, and cannot capture the dynamic evolution of soft interfaces under realistic operating conditions [22–25]. Critically, they fail to reproduce the electrochemical environment in which sensor performance is ultimately determined [26,27]. Complementary techniques such as quartz crystal microbalance with dissipation (QCM-D) and optical reflectometry provide valuable insight into mass uptake, viscoelastic properties, and film thickness during multilayer growth [28]. While these methods offer detailed structural and physicochemical information, they do not directly probe interfacial charge-transfer processes. In contrast, LbL-EC uniquely provides access to electrochemical descriptors of interfacial functionality that are directly relevant to biosensor performance [28–30].

LbL-EC directly addresses this gap. By monitoring the electrode–electrolyte interface under working conditions, LbL-EC translates morphological imperfections into functional consequences. Defects such as pinholes, loose packing, inhomogeneous redox distribution, or lateral molecular interactions, often invisible to imaging, manifest electrochemically as deviations from ideal Nernstian behaviour and frequently define the rate-limiting steps of sensor performance.

In this context, LbL-EC defines the benchmark strategy for monitoring the stepwise construction of EBs, offering high sensitivity to interfacial changes at each deposition step. This capacity is particularly effective in label-free architectures employing diffusional redox probes (DRP) such as $[Ru(NH_3)_6]^{3+/2+}$ or $[Fe(CN)_6]^{3-/4-}$, which sensitively transduce variations in interfacial charge transfer and surface accessibility [31–35]. The electrochemical response is inherently probe-dependent: cationic and anionic species interact differently with charged or permselective multilayers, yielding distinct voltammetric and impedance signatures. Consequently, LbL-EC readouts reflect both interfacial properties and probe–interface interactions rather than intrinsic characteristics alone. Probe selection should therefore consider reversibility (fast outer-sphere electron transfer), charge, size, and potential specific interactions with the film. The use of complementary probes can further improve the assessment of interfacial behaviour [36].

CV and EIS provide quantitative descriptors of interfacial processes, including peak current (p), formal potential (E°), heterogeneous electron transfer rate constant (k°), and charge transfer resistance (Rct) [37–40]. For example, nanomaterial interlayers typically enhance conductivity and expand the electroactive area (A), resulting in a higher Ip and reduced Rct. In contrast, blocking layers or biorecognition elements, such as antibodies and aptamers, partially shield the interface, resulting in decreased current and increased Rct [41], as illustrated in Figure 2.

The bare electrode (an electrode without any deposition and modification) can be approximated as an ideal reversible system (Nernstian), where current responses follow the Randles–Ševčík equation and parameters such as Ipa/Ipc ratio, ΔE, diffusion coefficient (D_0), and k° confirm rapid electron transfer (Figure 2a). Deviations from ideality, such as peak broadening, ΔE expansion, asymmetry (Ipa/Ipc ≠ 1), or the emergence of several peaks per redox event, reveal heterogeneous charge transfer pathways, arise upon biomolecule immobilization (Figure 2 b, d). Similarly, Nyquist plots reveal an increase in Rct and deviations from the canonical 45° Warburg slope, consistent with restricted probe diffusion and reduced electroactive area due to surface shielding by dense molecular layers (Figure 2c-e).

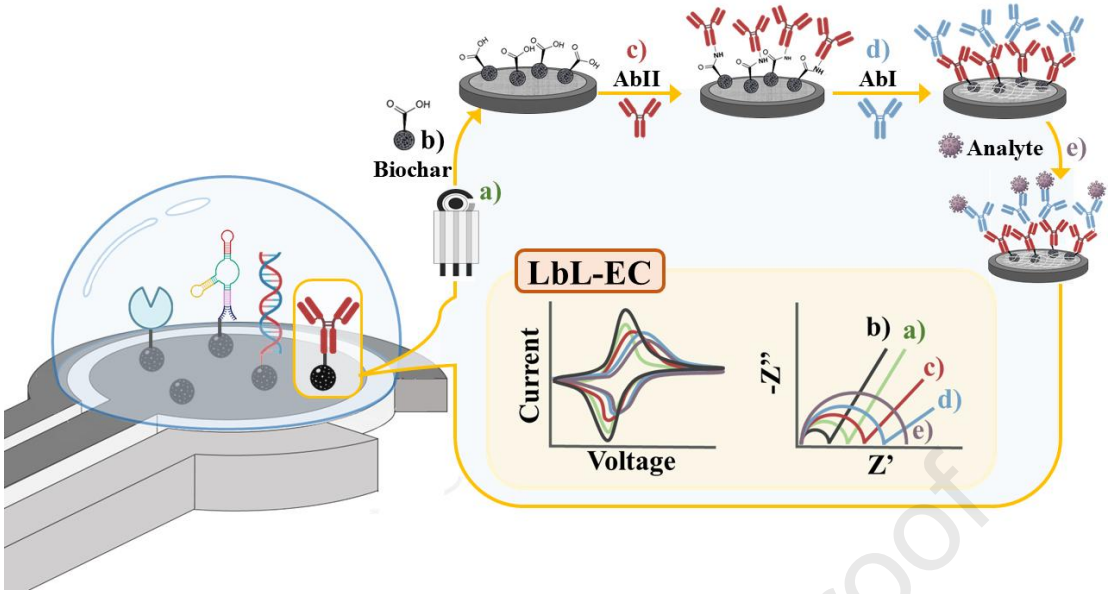

Figure 2. Application of LbL-EC techniques in the assembly and characterisation of immunosensors. Schematic illustration of a layer-by-layer (LbL) immunosensor assembly monitored by cyclic voltammetry (CV) and electrochemical impedance spectroscopy (EIS). a) SPE bare WE. b) WE modification with biochar, a sustainable carbon nanomaterial that acts both as an electrochemical enhancer (increasing Ip, reducing ΔE and Rct) and as an anchoring platform for bioreceptors. c) Covalent immobilisation of the secondary antibody (AbII) via EDC/NHS-mediated amide coupling. d) Immobilisation of the primary antibody (AbI). e) Target recognition, exemplified here by viral analyte binding. Adapted from Cancelliere et al. (2022)[42].

Beyond structural characterisation, LbL-EC enables the stepwise assessment of sensor robustness under environmental perturbations. Changes in pH, ionic strength, or buffer composition affect interfacial charge and organisation, which are reflected in the electrochemical response [43]. When DRPs are employed, CV and EIS signals arise from faradic processes that reflect probe-interface interactions under electrolyte conditions rather than the intrinsic sensing environment and should therefore be interpreted as diagnostic of interfacial behaviour. In contrast, measurements performed in supporting electrolytes without added redox species (buffer or KCl solutions) provide complementary, non-faradaic information on interfacial capacitance and intrinsic interfacial properties. As highlighted by Huffman et al. [36], this approach provides a powerful means of probing film stability under physiologically relevant conditions.

Despite its clear advantages, LbL-EC faces two critical limitations. First, it yields **global characterisation**: CV and EIS responses average over the entire interface, potentially masking nanoscale heterogeneities that SEM, TEM, or AFM readily detect [44]. Second, **non-ideal behaviours**, arising from disordered monolayers, incomplete coverage, or lateral molecular

interactions, complicate interpretation and demand expert modelling [45–48]. For this reason, hybrid approaches that integrate LbL-EC with imaging methods provide the most robust framework. Electrochemistry supplies stepwise functional readouts, while imaging validates structural uniformity. Together, they deliver the multiscale insight required to engineer multilayer architectures that are reliable, sensitive, and selective [49,50]. A comparative overview of these complementary methods is presented in Table 1.

Table 1. Overview of commonly employed techniques in the characterisation of multilayer sensor architectures.

Technique	Information	Advantages	Limitations
SEM / TEM	Morphology, defect sites, nanoscale structural detail	High-resolution structural imaging	Static snapshots; require vacuum; unsuitable for soft or hydrated architectures
STM / AFM	Surface topology, molecular packing density	Atomic- to nanoscale resolution	Surface-limited; no in-operando monitoring; extremely sensitive to environmental noise
CV / EIS (LbL-EC)	Charge transfer kinetics, layer homogeneity, interfacial dynamics	Stepwise, functional characterisation	Complex interpretation; spatial averaging masks nanoscale heterogeneity
Hybrid approaches	Integrated structural and functional readouts	Multiscale, comprehensive insight	Increased experimental complexity; requires multimodal expertise

3. LbL-EC in (Bio)sensing applications

While the theoretical aspects of LbL-EC have been previously discussed, this section delves into the application of LbL-EC, illustrating how this approach is currently being utilised in biosensing. EBs rely on the intimate coupling between a bioreceptor and a transducer, where the nature of the biological interface dictates selectivity, sensitivity, and stability. Bioreceptors encompass a broad spectrum of entities, ranging from nucleic acid–based probes (DNA, aptamers) and antibodies to enzymes and functional proteins, each exploiting distinct mechanisms of target recognition and signal amplification. Their immobilisation on conductive supports requires precise interfacial engineering to preserve biological activity while ensuring efficient electron transfer [51].

LbL-EC has proven particularly powerful in guiding this process. Unlike purely morphological approaches, LbL-EC enables real-time tracking of each assembly step, ensuring that nanomaterials, linker chemistries, and biomolecules are integrated in an ordered and functional manner. This has enabled the development of diverse sensing platforms, including aptasensors for toxins and nucleic acids, DNA-based sensors for genetic biomarkers, enzyme electrodes for metabolite monitoring, and antibody-based immunosensors for proteins, cytokines, and viral antigens.

Recent reports demonstrate how LbL-EC supports the rational optimisation of multilayer architectures by correlating interfacial charge transfer behaviour with recognition efficiency. The incorporation of nanomaterials such as biochar, graphene, carbon nanotubes, and metallic nanoparticles further highlights its role in enhancing electroactive area, conductivity, and biomolecule anchoring. These advances highlight the ability of LbL-EC not only to validate biosensor construction, a powerful technique for constructing high-performance biosensors, but also to predict and enhance analytical performance under working conditions. Table 2 summarises the most innovative applications of LbL-EC in biosensing reported over the last four years, highlighting the diversity of targets, materials, and strategies explored. An example of LbL-EC application in biosensor construction is reported by Barman et al. (2021) [52] to develop an impedimetric immunosensor for interleukin-6 detection; in their work, Black Phosphorus was leveraged and embedded in PAMI to modify the electrode surface to enhance electrochemical performance and to allow antibody covalent immobilization. EIS and CV tracked a rise in R_{CT} and a decrease in Peak current at each stage of the sensor manufacturing process, including BP-PAMI, antibody immobilization, blocking, and IL-6 detection. This allowed for the adjustment of parameters including surface coverage and blocking efficiency. LbL-EC by itself cannot be used to study the deterioration of BP and its surface inhomogeneity. Therefore, preliminary AFM, TEM, and Raman analyses are crucial to the development of the biosensor in this work. Although LbL-EC provides important information about the behavior under operating conditions, it often needs to be utilized in combination with structural imaging methods to ensure complete material characterization. Thanks to this integrated approach, the final biosensor exhibited excellent analytical performance, with a linear detection range between 0.003 and 75 ng/mL and a limit of detection (LOD) as low as 1 pg/mL for IL-6.

Sometimes, the interpretation of electrochemical signals requires a deeper understanding of electrochemical techniques and phenomena. Particularly, in densely packed or organized layers, some molecular effects can disturb the expected electrochemical signal, potentially leading to misinterpretation using LbL-EC approach. For example, Duffin et al. (2019) [53] demonstrated that the electric field in alkyl-ferrocenylalkanethiolate SAMs is not uniform. Their application of LbL-EC demonstrated that supramolecular organization had an impact on the local potential distribution within the film, leading to peaks overlapping in CV. These findings indicate that the uniform electrode potential assumption is not always accurate, and specialized personnel are needed to avoid errors in interpreting kinetic and structural parameters extracted from CV and EIS data.

Additionally, an analysis of ferrocenylalkanethiolate SAMs on gold electrodes was reported by Tian et al. (2012) [54], which demonstrates that, even in well-formed layers, peak broadening, splitting, and shifts in CV responses arise when intermolecular interactions differ between the oxidised and reduced states of immobilised species. In such systems, electrostatic interactions within the film and at the interface often dominate the thermodynamic response, leading to a distribution of formal potentials and non-ideal voltammetric behaviour. This highlights that deviations from ideal CV and EIS patterns may originate from nanoscale molecular organisation and interfacial heterogeneity, rather than necessarily indicating poor layer assembly.

To overcome these challenges, artificial intelligence (AI) and machine learning (ML) have recently emerged as powerful tools in complex dataset interpretation. Rather than focusing solely on classification, these approaches enable the extraction of hidden features associated with interfacial heterogeneity and non-ideal electrochemical behaviour. In the context of LbL-EC, deviations from ideal CV and EIS responses, such as peak broadening, asymmetry, or distributed charge-transfer resistance, can be difficult to interpret using conventional models. Our recent work illustrates this potential, demonstrating how ML-based approaches can resolve overlapping electrochemical signals and reveal hidden features in complex voltammetric datasets [55].

Data-driven methods, including convolutional neural networks (CNNs) and advanced signal transformations (Gramian angular fields), offer a complementary framework to identify patterns related to non-uniform surface coverage, heterogeneous electron-transfer pathways, and interfacial disorder. Such features can be translated into electrochemical descriptors that inform the optimisation of multilayer assembly. In this way, AI-assisted analysis moves LbL-EC beyond qualitative interpretation, enabling a more quantitative and predictive understanding of interfacial processes and supporting the rational design of reproducible and better-performing biosensors

Table 2. Representative examples of LbL-EC applied to EB development over the last three years. The table highlights the diversity of targets (proteins, nucleic acids, toxins, metabolites, pathogens), the biorecognition strategies employed (antibodies, aptamers, enzymes, DNA probes), and the integration of nanostructured materials for enhanced performance. Reported limits of detection (LOD) and complementary non-electrochemical characterisation techniques are included to illustrate how LbL-EC provides functional insights that bridge structural analysis and device optimisation.

Target	Type of biosensor	Layers materials	LbL-EC technique	Not LbL-EC technique	LOD	Reference
IL-6	**Immuno.**	**BP-PAMI, Abs**	**CV EIS**	**AFM TEM**	**1 pg/ml**	[52]

				Zeta Potential XPS Raman XRD SEM TEM UV-vis		
OLA	**Immuno.**	**GO, AgNPs, PEI, AuNPs, Abs**	**CV EIS DPV**		**4.8 pg/ml**	[56]
CYFRA21-1	**Immuno.**	**Si_3N_4/MoS_2–MWCNTs, Abs, MMSNs@AuNPs**	**CV EIS DPV**	**XRD SEM TEM XRD XPS FTIR**	**2.0 fg/ml**	[57]
VEGF	**Immuno.**	**rGO, Abs**	**CV SWV**	**SEM Raman XPS**	**0.1 pg/ml**	[58]
SARS-CoV-2 S protein	**Immuno.**	**Cu2O NCs, Prot A, Abs**	**CV, EIS**		**0.04 fg/ml**	[59]
IL-1β	**Immuno.**	**Au–Ag–MoS_2-rGO, peptide**	**CV EIS SWV**	**XRD XPS FE-SEM**	**2.4 pM**	[60]
TNF- α	**Immuno.**	**MoS_2 nf, Abs**	**CV EIS**	**XRD SEM TEM AFM Raman**	**0.202 pg/ml**	[61]
Ochratoxin A	**Immuno.**	**MBA, Abs**	**CV EIS**	**AFM**	**0.19 ng/ml**	[62]
α-synuclein protein	**Immuno.**	**AuNPs, Abs**	**EIS SWV DPV CA**	**DLS AFM FE-SEM EDX**	**4 ng/ml**	[63]
β-Amyloid1-42	**Immuno.**	**PtCOCuNPs/rGO, Abs**	**CV EIS CA**	**TEM XPS EDX SEM**	**3.5 fg/ml**	[64]
CEA, CA125, CA153, CA199	**Immuno.**	**PBNCs, cryogel, Abs**	**CV EIS**	**SEM AFM**	**CEA: 0.79 pg/mL, CA125: 0.37 mU/mL, CA153: 0.49 mU/mL,**	[65]

					CA199: 0.48 mU/mL	
Quinalphos	Immuno.	PVA/Gelatin–AuNPs nanofiber, nanobody	EIS	FTIR SEM AFM	50.74 pg/ml	[66]
PSA	Immuno.	Fe-Cu LDH, rGO, Abs	CV EIS	FE-SEM EDX XRD FTIR	63.24 fg/ml	[67]
Ochratoxin A	Immuno.	AuNPs, Abs	EIS	EDS SEM AFM Raman	0.15ng/ml	[68]
α-synuclein	Immuno.	SWCNTs AuNPs, Abs	CV EIS SWV	SEM	4.1 pg/ml	[69]
CA125	Immuno.	CuCo-ONSs@AuNPs, Abs	CV EIS DPV	SEM TEM XRD XPS	3.9×10^{-8} U/mL	[70]
Lymphoma cancer cells	Immuno.	AuNPs@DTSP, BA, Ab, BSA	EIS	TEM FT-IR	62 cell/ml	[71]
CEA	Apta.	KMPPH, aptamer	EIS CV DPV	XRD FT-IR TEM SEM	0.41 pg/ml	[72]
AFB1	Apta.	Aptamer, GNs, PSCOOH NPs, PDDA	CV EIS	FE-SEM TEM	0.002 ng/ml	[73]
Leptin	Apta.	TiO2NPs, AuNPs, Aptamer	CV EIS	SEM	0.312 pg/ml	[74]
HepG2 cells	Apta.	AuNPs, aptamer, PtNPs	CV EIS DPV	DLS SEM TEM	15 cell/ml	[75]
HPV mRNA	Apta.	AuNPs, Hairpin, PLL-*g*-Dex	CV EIS DPV	SEM	0.88pM	[76]
CA15-3	Apta.	AuTF, rGO-MoS_2	CV EIS	XRD FE-SEM EDS	0.3 U/ml	[77]

viral S protein	**Apta.**	**AuNPs, aptamer**	**CV DPV**	**SEM**	**91.1pM**	[78]
Growth Factor-1	**Apta-Immuno.**	**TDN, Abs**	**CV EIS SWV**	**PAGE AFM TEM UV-vis**	**0.47 fM**	[79]
***stx1* gene**	**DNA**	**AuNPs, Chitosan, DNA-probe**	**CV EIS SWV**	**FM SEM EDX**	**100 aM**	[80]
miRNA-21	**DNA**	**rGO, AuNPs, DNA probe**	**CV EIS DPV**	**XRD FTIR EDS XPS**	**1.73 pM**	[81]
CA15-3	**Enz.**	**rGO-AuNPs, Abs, HRP-Abs**	**CV EIS SWV**	**SEM EDS**	**0.08 fg/ml**	[82]
CA125	**Enz.**	**CS-AuNP/MWCNT/G, Abs, AuNPs-Lox-Abs**	**CV EISCA**	**XRD, DLS, SEM,TEM, UV-Vis**	**0.002 U/mL**	[83]
cancerous exosomes and thrombin	**Enz.**	**GOx/HRP DFs, aptamer**	**CV EIS DPV**	**SEM TEM DLS**	**Exosomes: $1.02 \cdot 10^3$ particles/µL Thrombin: 12.77 fM,**	[84]
8-OHdG	**Other**	**Fe_3AlC_2 nanoflakes**	**CV DPV CC**	**XRD SEM**	**50 pM**	[85]

Achronyms: Immunosensor (Immuno), Aptamer (Apta.), Enzyme (Enz.) Cyclic Voltammetry (CV), Electrochemical impedance spectroscopy (EIS), differential pulsed voltammetry (DPV), Square wave voltammetry (SWV), Chronoamperometry (CA), Chronocoulometry (CC), Scanning Electron Microscopy (SEM), Transmission Electron Microscopy (TEM), Atomic Force Microscopy (AFM), X-ray Photoelectron Spectroscopy (XPS), X-ray Diffraction (XRD), Fourier Transform Infrared Spectroscopy (FT-IR), Field Emission Scanning Electron Microscopy (FE-SEM), Energy Dispersive X-ray Spectroscopy (EDX), Energy Dispersive Spectroscopy (EDS), Dynamic Light Scattering (DLS), Polyacrylamide Gel Electrophoresis (PAGE), Fluorescence Microscopy (FM), black phosphorene-polyallylamine (BP-PAMI), Antibodies (Abs), Graphene oxide (GO), Silver Nanoparticles (AgNPs), Gold Nanoparticles (AuNPs), Polyethyleneimine (PEI), Multi-Walled Carbon Nanotubes (MWCNTs), magnetic mesoporous silica nanoparticles@gold nanoparticles (MMSNs@AuNPs), reduced Graphene Oxide (rGO), nanocubes (NCs), Protein A (Prot A), nanoflower (nf), Mercaptobenzoic acid (MBA), Prussian Blue Nano Cubes (PBNCs), Polyvinyl alcohol (PVA), layered double hydroxide (LDH), nanogold-functionalized copper-cobalt oxide nanosheets (CuCo-ONSs@AuNPs), 3,3′-dithiodipropionic acid (DTSP), Boronic Acid (BA), Bovine Serum Albumin (BSA), K-MXene-PEDOT:PSS-PNIPAM hydrogels (KMPPH), N-doped graphene nanosheets (GNs), Polystyrene (PS), Poly(diallyl dimethylammonium chloride) solution (PDDA), Poly($_L$-lysine)-*graft*-dextran (PLL-*g*-Dex), gold thin film (AuTF), tetrahedral DNA nanostructure (TDN), Horseradish Peroxidase (HRP), Chitosan-gold nanoparticle (CS-AuNP), lactate oxidase (LOx), DNA flowers (DFs), Interleukin-6 (IL-6), Olaquindox (OLA), vascular endothelial growth factor (VEGF), interleukin-1beta (IL-1β), Tumor Necrosis Factor-α (TNF-α), carcinoembryonic

antigen (CEA), carbohydrate antigen 125 (CA125), carbohydrate antigen 153 (CA153), carbohydrate antigen 199 (CA199), 8-hydroxy-2′-deoxyguanosine (8OHdG)

Conclusions, Challenges and Future Perspectives

LbL-EC has emerged as a powerful framework for the controlled fabrication and interrogation of multilayered biosensor interfaces. By enabling stepwise electrochemical monitoring of assembly processes, it provides access to key interfacial descriptors, including charge-transfer kinetics, surface accessibility, and heterogeneity, that underpin sensor behaviour. In this context, LbL-EC bridges the gap between structural organisation and functional response, offering capabilities that complement, rather than replace, conventional imaging techniques such as SEM, TEM, and AFM.

Nevertheless, significant challenges remain. Electrochemical responses intrinsically average over the entire electrode interface, potentially masking nanoscale heterogeneities that critically influence device performance. Furthermore, non-ideal voltammetric and impedance patterns arising from disordered assemblies, lateral molecular interactions, or uneven coverage often require advanced expertise and sophisticated modelling to be interpreted accurately. These complexities reinforce the necessity of hybrid characterisation strategies, where LbL-EC is coupled with high-resolution imaging and spectroscopic methods to correlate morphology with function across multiple length scales.

Looking forward, the integration of **LbL-EC with AI** represents a powerful route to advance the field. Data-driven methods can extract electrochemical descriptors from complex, non-ideal signals, revealing interfacial features beyond conventional analysis. By linking electrochemical response to design parameters, AI-assisted LbL-EC can enable more rational and reproducible optimisation of multilayer architectures. [55]. This synergy will accelerate the development of next-generation biosensors that are not only more selective, sensitive, and durable, but also capable of autonomous optimisation and self-diagnosis, propelling their translation into real-world healthcare, environmental, and point-of-care applications.

CRediT authorship contribution statement.

R. Cancelliere: Writing–original draft, Writing – review & editing, Visualisation, Supervision, Conceptualisation, Funding acquisition. **A. Licheri**: Writing – original draft, Visualisation, Conceptualisation. **E. Paialunga**: Visualisation. **L. Micheli**: Writing – review & editing, Visualisation, Supervision, Funding Acquisition.

Declaration of competing interest

The authors declare that they have no known competing financial interests or personal relationships that could have appeared to influence the work reported in this paper.

Acknowledgement

This was supported by the Regione Lazio-funded project SFIDE grant n. FISR2020IP_02585; "Environmental Sensing With Artificial Intelligence (MUR - PRIN_2022 - SENS-AI -CUP: E53D23000830006) and Grant MUR Dipartimento di Eccellenza 2023-27 X-CHEM project "eXpanding CHEMistry: implementing excellence in research and teaching". PNRR-POR H2 supported by the National Recovery and Resilience Plan (NEXT GENERATION EU, CUP:183C22001170006)

References

[1] S. Menon, M.R. Mathew, S. Sam, K. Keerthi, K.G. Kumar, Recent advances and challenges in electrochemical biosensors for emerging and re-emerging infectious diseases, J. Electroanal. Chem. 878 (2020) 114596. https://doi.org/10.1016/j.jelechem.2020.114596.

[2] A.L. Yost, S. Shahsavari, G.M. Bradwell, R. Polak, F. Fachin, R.E. Cohen, G.H. McKinley, M. Toner, M.F. Rubner, B.L. Wardle, Layer-by-layer functionalized nanotube arrays: A versatile microfluidic platform for biodetection, Microsyst. Nanoeng. 1 (2015) 15037. https://doi.org/10.1038/micronano.2015.37.

[3] J. Wu, H. Liu, W. Chen, B. Ma, H. Ju, Device integration of electrochemical biosensors, Nat. Rev. Bioeng. 1 (2023) 346–360. https://doi.org/10.1038/s44222-023-00032-w.

[4] M.H. Iqbal, H. Kerdjoudj, F. Boulmedais, Protein-based layer-by-layer films for biomedical applications, Chem. Sci. 15 (2024) 9408–9437. https://doi.org/10.1039/D3SC06549A.

[5] W. Zhao, J. Xu, H. Chen, Electrochemical Biosensors Based on Layer-by-Layer Assemblies, Electroanalysis 18 (2006) 1737–1748. https://doi.org/10.1002/elan.200603630.

[6] R.M. Iost, F.N. Crespilho, Layer-by-layer self-assembly and electrochemistry: Applications in biosensing and bioelectronics, Biosens. Bioelectron. 31 (2012) 1–10. https://doi.org/10.1016/j.bios.2011.10.040.

[7] Y.B. Cui, Z. Sun, M. Qing, L.D. Yu, H. Yan, H.Q. Luo, N.B. Li, A "signal on" photoelectrochemical biosensor for miRNA-21 detection based on layer-by-layer assembled n-n type Bi2S3@CdIn2S4 heterojunction, Sens. Actuators B Chem. 373 (2022) 132702. https://doi.org/10.1016/j.snb.2022.132702.

[8] Y. Ding, Y. Zhang, C. Huang, J. Wang, H. Li, X. Wang, An electrochemical biosensor based on phage-encoded protein RBP 41 for rapid and sensitive detection of Salmonella, Talanta 270 (2024) 125561. https://doi.org/10.1016/j.talanta.2023.125561.

[9] K. Teeparuksapun, M. Hedström, B. Mattiasson, A Sensitive Capacitive Biosensor for Protein a Detection Using Human IgG Immobilized on an Electrode Using Layer-by-Layer Applied Gold Nanoparticles, Sensors 22 (2021) 99. https://doi.org/10.3390/s22010099.

[10] R. Boukherroub, S. Szunerits, The Future of Nanotechnology-Driven Electrochemical and Electrical Point-of-Care Devices and Diagnostic Tests, Annu. Rev. Anal. Chem. 17 (2024) 173–195. https://doi.org/10.1146/annurev-anchem-061622-012029.

[11] H. Duan, S. Peng, S. He, S. Tang, K. Goda, C.H. Wang, M. Li, Wearable Electrochemical Biosensors for Advanced Healthcare Monitoring, Adv. Sci. 12 (2025) 2411433. https://doi.org/10.1002/advs.202411433.

[12] D. Wachholz Junior, P.B. Deroco, B.M. Hryniewicz, L.T. Kubota, Strategies for Electrochemical Point-of-Care Biosensors, Annu. Rev. Anal. Chem. 18 (2025) 307–333. https://doi.org/10.1146/annurev-anchem-071124-103739.

[13] K. Sankar, U. Kuzmanović, S.E. Schaus, J.E. Galagan, M.W. Grinstaff, Strategy, Design, and Fabrication of Electrochemical Biosensors: A Tutorial, ACS Sens. 9 (2024) 2254–2274. https://doi.org/10.1021/acssensors.4c00043.
[14] M. Barawi, C.A. Mesa, L. Collado, I.J. Villar-García, F. Oropeza, V.A. De La Peña O'Shea, M. García-Tecedor, Latest advances in *in situ* and *operando* X-ray-based techniques for the characterisation of photoelectrocatalytic systems, J. Mater. Chem. A 12 (2024) 23125–23146. https://doi.org/10.1039/D4TA03068K.
[15] H. Nevison-Andrews, A.W. Robertson, Challenges and opportunities in *operando* electrochemical liquid cell TEM, Chem. Phys. Rev. 6 (2025) 031302. https://doi.org/10.1063/5.0267692.
[16] H. Alnoor, A. Elsukova, J. Palisaitis, I. Persson, E.N. Tseng, J. Lu, L. Hultman, P.O.Å. Persson, Exploring MXenes and their MAX phase precursors by electron microscopy, Mater. Today Adv. 9 (2021) 100123. https://doi.org/10.1016/j.mtadv.2020.100123.
[17] G. Li, H. Zhang, Y. Han, Applications of Transmission Electron Microscopy in Phase Engineering of Nanomaterials, Chem. Rev. 123 (2023) 10728–10749. https://doi.org/10.1021/acs.chemrev.3c00364.
[18] M. Gao, Y. Jang, L. Ding, Y. Gao, S. Dai, Z. Dai, G. Yu, W. Yang, F. Wang, Mechanism of the noncatalytic oxidation of soot using in situ transmission electron microscopy, Nat. Commun. 14 (2023) 6256. https://doi.org/10.1038/s41467-023-41726-4.
[19] K. Iwata, S. Yamazaki, P. Mutombo, P. Hapala, M. Ondráček, P. Jelínek, Y. Sugimoto, Chemical structure imaging of a single molecule by atomic force microscopy at room temperature, Nat. Commun. 6 (2015) 7766. https://doi.org/10.1038/ncomms8766.
[20] A. Shiotari, Y. Sugimoto, Ultrahigh-resolution imaging of water networks by atomic force microscopy, Nat. Commun. 8 (2017) 14313. https://doi.org/10.1038/ncomms14313.
[21] O. Stetsovych, M. Todorović, T.K. Shimizu, C. Moreno, J.W. Ryan, C.P. León, K. Sagisaka, E. Palomares, V. Matolín, D. Fujita, R. Perez, O. Custance, Atomic species identification at the (101) anatase surface by simultaneous scanning tunnelling and atomic force microscopy, Nat. Commun. 6 (2015) 7265. https://doi.org/10.1038/ncomms8265.
[22] F.M. Ross, Opportunities and challenges in liquid cell electron microscopy, Science 350 (2015) aaa9886. https://doi.org/10.1126/science.aaa9886.
[23] Z. Han, A.E. Porter, In situ Electron Microscopy of Complex Biological and Nanoscale Systems: Challenges and Opportunities, Front. Nanotechnol. 2 (2020) 606253. https://doi.org/10.3389/fnano.2020.606253.
[24] E. Nogales, J. Mahamid, Bridging structural and cell biology with cryo-electron microscopy, Nature 628 (2024) 47–56. https://doi.org/10.1038/s41586-024-07198-2.
[25] D. Llorens Rauret, A. Garzón Manjón, J. Arbiol, Advances in in situ and operando TEM: From basic catalysis to industry-relevant reactions and future directions, Matter 8 (2025) 102139. https://doi.org/10.1016/j.matt.2025.102139.
[26] K. Chen, A.S. Barnard, Advancing electron microscopy using deep learning, J. Phys. Mater. 7 (2024) 022001. https://doi.org/10.1088/2515-7639/ad229b.
[27] H. Stahlberg, T. Walz, Molecular Electron Microscopy: State of the Art and Current Challenges, ACS Chem. Biol. 3 (2008) 268–281. https://doi.org/10.1021/cb800037d.
[28] J. Rickert, A. Brecht, W. Göpel, Quartz crystal microbalances for quantitative biosensing and characterizing protein multilayers, Biosens. Bioelectron. 12 (1997) 567–575. https://doi.org/10.1016/S0956-5663(96)00077-2.
[29] A.D. Easley, T. Ma, C.I. Eneh, J. Yun, R.M. Thakur, J.L. Lutkenhaus, A practical guide to quartz crystal microbalance with dissipation monitoring of thin polymer films, J. Polym. Sci. 60 (2022) 1090–1107. https://doi.org/10.1002/pol.20210324.
[30] A. Darbandi, M. Lettieri, G. Leone, A. Magnani, M. Consumi, Nanostructured quartz crystal microbalance biosensors: Emerging frontiers in diagnostic applications, Microchem. J. 224 (2026) 117635. https://doi.org/10.1016/j.microc.2026.117635.
[31] B. Liu, W. Lu, Y. Huang, X. Zhang, X. Yuan, A label-free electrochemical sensor for the detection of two kinds of targets based on CRISPR/Cas12a system, Sens. Actuators B Chem. 406 (2024) 135406. https://doi.org/10.1016/j.snb.2024.135406.

[32] R. Cancelliere, E. Paialunga, A. Grattagliano, L. Micheli, Label-free electrochemical immunosensors: A practical guide, TrAC Trends Anal. Chem. 180 (2024) 117949. https://doi.org/10.1016/j.trac.2024.117949.
[33] C.C. Mayorga-Martinez, A. Chamorro-Garcia, A. Merkoçi, Electrochemical Impedance Spectroscopy (bio)sensing through hydrogen evolution reaction induced by gold nanoparticles, Biosens. Bioelectron. 67 (2015) 53–58. https://doi.org/10.1016/j.bios.2014.05.066.
[34] C.C. Mayorga-Martinez, A. Chamorro-García, L. Serrano, L. Rivas, D. Quesada-Gonzalez, L. Altet, O. Francino, A. Sánchez, A. Merkoçi, An iridium oxide nanoparticle and polythionine thin film based platform for sensitive Leishmania DNA detection, J. Mater. Chem. B 3 (2015) 5166–5171. https://doi.org/10.1039/C5TB00545K.
[35] H. Zhang, Z. Sun, K. Sun, Q. Liu, W. Chu, L. Fu, D. Dai, Z. Liang, C.-T. Lin, Electrochemical Impedance Spectroscopy-Based Biosensors for Label-Free Detection of Pathogens, Biosensors 15 (2025) 443. https://doi.org/10.3390/bios15070443.
[36] B.L. Huffman, A.R.C. Bredar, J.L. Dempsey, Origins of non-ideal behaviour in voltammetric analysis of redox-active monolayers, Nat. Rev. Chem. 8 (2024) 628–643. https://doi.org/10.1038/s41570-024-00629-8.
[37] E.P. Randviir, C.E. Banks, Electrochemical impedance spectroscopy: an overview of bioanalytical applications, Anal. Methods 5 (2013) 1098. https://doi.org/10.1039/c3ay26476a.
[38] E.P. Randviir, C.E. Banks, A review of electrochemical impedance spectroscopy for bioanalytical sensors, Anal. Methods 14 (2022) 4602–4624. https://doi.org/10.1039/D2AY00970F.
[39] H.S. Magar, R.Y.A. Hassan, A. Mulchandani, Electrochemical Impedance Spectroscopy (EIS): Principles, Construction, and Biosensing Applications, Sensors 21 (2021) 6578. https://doi.org/10.3390/s21196578.
[40] S. Wang, J. Zhang, O. Gharbi, V. Vivier, M. Gao, M.E. Orazem, Electrochemical impedance spectroscopy, Nat. Rev. Methods Primer 1 (2021) 41. https://doi.org/10.1038/s43586-021-00039-w.
[41] S.C. Barman, Y. Jin, J.K. El-Demellawi, S. Thomas, N. Wehbe, Y. Lei, M.K. Hota, X. Xu, E.A. Hasan, O.F. Mohammed, O.M. Bakr, D. Alsulaiman, H.N. Alshareef, Antibody-functionalized MXene-based electrochemical biosensor for point-of-care detection of vitamin D deficiency, Commun. Mater. 6 (2025) 31. https://doi.org/10.1038/s43246-025-00756-9.
[42] R. Cancelliere, A. Di Tinno, A.M. Di Lellis, G. Contini, L. Micheli, E. Signori, Cost-effective and disposable label-free voltammetric immunosensor for sensitive detection of interleukin-6, Biosens. Bioelectron. 213 (2022) 114467. https://doi.org/10.1016/j.bios.2022.114467.
[43] R.A. Wong, Y. Yokota, M. Wakisaka, J. Inukai, Y. Kim, Probing consequences of anion-dictated electrochemistry on the electrode/monolayer/electrolyte interfacial properties, Nat. Commun. 11 (2020) 4194. https://doi.org/10.1038/s41467-020-18030-6.
[44] T. Ma, D.V. Baker, G. Martinez-Blanco, D. Bizzotto, An EIS study of the heterogeneity of redox labeled DNA SAMs on gold before and after hybridization, Electrochimica Acta 517 (2025) 145747. https://doi.org/10.1016/j.electacta.2025.145747.
[45] A.Ch. Lazanas, M.I. Prodromidis, Electrochemical Impedance Spectroscopy–A Tutorial, ACS Meas. Sci. Au 3 (2023) 162–193. https://doi.org/10.1021/acsmeasuresciau.2c00070.
[46] A. López-Marzo, M. Mas-Torrent, Bioreceptors' immobilization by hydrogen bonding interactions and differential pulse voltammetry for completely label-free electrochemical biosensors, Microchim. Acta 191 (2024) 669. https://doi.org/10.1007/s00604-024-06738-x.
[47] Y. Zhao, J. Chen, Z. Hu, Y. Chen, Y. Tao, L. Wang, L. Li, P. Wang, H.-Y. Li, J. Zhang, J. Tang, H. Liu, All-solid-state SARS-CoV-2 protein biosensor employing colloidal quantum dots-modified electrode, Biosens. Bioelectron. 202 (2022) 113974. https://doi.org/10.1016/j.bios.2022.113974.
[48] J.A. Ribeiro, P.A.S. Jorge, Applications of electrochemical impedance spectroscopy in disease diagnosis—A review, Sens. Actuators Rep. 8 (2024) 100205. https://doi.org/10.1016/j.snr.2024.100205.
[49] N. Kalita, S. Gogoi, S.D. Minteer, P. Goswami, Advances in Bioelectrode Design for Developing Electrochemical Biosensors, ACS Meas. Sci. Au 3 (2023) 404–433. https://doi.org/10.1021/acsmeasuresciau.3c00034.

[50] L. Guo, Y. Zhao, Q. Huang, J. Huang, Y. Tao, J. Chen, H.-Y. Li, H. Liu, Electrochemical protein biosensors for disease marker detection: progress and opportunities, Microsyst. Nanoeng. 10 (2024) 65. https://doi.org/10.1038/s41378-024-00700-w.

[51] S. Gao, J.M. Guisán, J. Rocha-Martin, Oriented immobilization of antibodies onto sensing platforms - A critical review, Anal. Chim. Acta 1189 (2022) 338907. https://doi.org/10.1016/j.aca.2021.338907.

[52] S. Chandra Barman, M. Sharifuzzaman, M.A. Zahed, C. Park, S.H. Yoon, S. Zhang, H. Kim, H. Yoon, J.Y. Park, A highly selective and stable cationic polyelectrolyte encapsulated black phosphorene based impedimetric immunosensor for Interleukin-6 biomarker detection, Biosens. Bioelectron. 186 (2021) 113287. https://doi.org/10.1016/j.bios.2021.113287.

[53] T.J. Duffin, N. Nerngchamnong, D. Thompson, C.A. Nijhuis, Direct measurement of the local field within alkyl-ferrocenyl-alkanethiolate monolayers: Importance of the supramolecular and electronic structure on the voltammetric response and potential profile, Electrochimica Acta 311 (2019) 92–102. https://doi.org/10.1016/j.electacta.2019.04.041.

[54] H. Tian, Y. Dai, H. Shao, H.-Z. Yu, Modulated Intermolecular Interactions in Ferrocenylalkanethiolate Self-Assembled Monolayers on Gold, J. Phys. Chem. C 117 (2013) 1006–1012. https://doi.org/10.1021/jp310012v.

[55] R. Cancelliere, M. Molinara, A. Licheri, A. Maffucci, L. Micheli, Artificial intelligence-assisted electrochemical sensors for qualitative and semi-quantitative multiplexed analyses, Digit. Discov. 4 (2025) 338–342. https://doi.org/10.1039/D4DD00318G.

[56] D. Liu, A. Wang, J. Zhou, X. Wang, H. Liu, P. Ding, Y. Zhang, X. Zhu, Y. Zhou, G. Zhang, A label-free electrochemical immunosensor based on AuNPs/GO-PEI-Ag-Nf for olaquindox detection in feedstuffs, Microchem. J. 177 (2022) 107287. https://doi.org/10.1016/j.microc.2022.107287.

[57] M.L. Yola, N. Atar, N. Özcan, A novel electrochemical lung cancer biomarker cytokeratin 19 fragment antigen 21-1 immunosensor based on Si_3N_4 /MoS_2 incorporated MWCNTs and core–shell type magnetic nanoparticles, Nanoscale 13 (2021) 4660–4669. https://doi.org/10.1039/D1NR00244A.

[58] R. Elshafey, P. Brisebois, H. Abdulkarim, R. Izquierdo, A.C. Tavares, M. Siaj, Effect of Graphene Oxide Sheet Size on the Response of a Label-free Voltammetric Immunosensor for Cancer Marker VEGF, Electroanalysis 32 (2020) 2205–2212. https://doi.org/10.1002/elan.202000065.

[59] Z. Rahmati, M. Roushani, H. Hosseini, H. Choobin, Electrochemical immunosensor with Cu2O nanocube coating for detection of SARS-CoV-2 spike protein, Microchim. Acta 188 (2021) 105. https://doi.org/10.1007/s00604-021-04762-9.

[60] H.J. Yang, C.V. Raju, C.-H. Choi, J.P. Park, Electrochemical peptide-based biosensor for the detection of the inflammatory disease biomarker, interleukin-1beta, Anal. Chim. Acta 1295 (2024) 342287. https://doi.org/10.1016/j.aca.2024.342287.

[61] S. Sri, D. Chauhan, G.B.V.S. Lakshmi, A. Thakar, P.R. Solanki, MoS2 nanoflower based electrochemical biosensor for TNF alpha detection in cancer patients, Electrochimica Acta 405 (2022) 139736. https://doi.org/10.1016/j.electacta.2021.139736.

[62] R. Cancelliere, D. Albano, B. Brugnoli, K. Buonasera, G. Leo, A. Margonelli, G. Rea, Electrochemical and morphological layer-by-layer characterization of electrode interfaces during a label-free impedimetric immunosensor build-up: The case of ochratoxin A, Appl. Surf. Sci. 567 (2021) 150791. https://doi.org/10.1016/j.apsusc.2021.150791.

[63] E.D. Aminabad, A. Mobed, M. Hasanzadeh, M.A. Hosseinpour Feizi, R. Safaralizadeh, F. Seidi, Sensitive immunosensing of α-synuclein protein in human plasma samples using gold nanoparticles conjugated with graphene: an innovative immuno-platform towards early stage identification of Parkinson's disease using point of care (POC) analysis, RSC Adv. 12 (2022) 4346–4357. https://doi.org/10.1039/D1RA06437A.

[64] Y. Wang, P. Wang, Z. Zhao, S. Ye, W. Wang, Q. Liu, Y. Li, D. Zhang, Y. Li, A label-free electrochemical immunosensor based on PtCoCu PNPs/NB-rGO as a dual signal amplification platform for sensitive detection of β-Amyloid1-42, Bioelectrochemistry 152 (2023) 108405. https://doi.org/10.1016/j.bioelechem.2023.108405.

[65] S. Kongkaew, S. Cotchim, P. Kanatharana, P. Thavarungkul, W. Limbut, Disposable label-free electrochemical immunosensor based on prussian blue nanocubes for four breast cancer tumor markers, Talanta 255 (2023) 124229. https://doi.org/10.1016/j.talanta.2022.124229.

[66] J. Hu, P. Wen, Y. Wang, J. Yang, Z. Xiao, Z. Xu, Y. Shen, H. Wang, B.D. Hammock, Fabrication of a label-free electrochemical immunosensor by functionalized nanofiber membrane for the ultrasensitive detection of quinalphos, Food Control 162 (2024) 110423. https://doi.org/10.1016/j.foodcont.2024.110423.
[67] Y. Ghasemi, M. Sadeghi, H. Ehzari, H. Derakhshankhah, Label-free electrochemical immunosensor based on antibody-immobilized Fe-Cu layered double hydroxide nanosheetas an electrochemical probe for the detection of ultra trace amount of prostate cancer biomarker (PSA), Microchem. J. 195 (2023) 109460. https://doi.org/10.1016/j.microc.2023.109460.
[68] J.P. De Oliveira, F. Burgos-Flórez, I. Sampaio, P. Villalba, V. Zucolotto, Label-free electrochemical immunosensor for Ochratoxin a detection in coffee samples, Talanta 260 (2023) 124586. https://doi.org/10.1016/j.talanta.2023.124586.
[69] P. Carneiro, J.A. Loureiro, C. Delerue-Matos, S. Morais, M.D.C. Pereira, Nanostructured label–free electrochemical immunosensor for detection of a Parkinson's disease biomarker, Talanta 252 (2023) 123838. https://doi.org/10.1016/j.talanta.2022.123838.
[70] W. Mu, C. Wu, F. Wu, H. Gao, X. Ren, J. Feng, M. Miao, H. Zhang, D. Chang, H. Pan, Ultrasensitive and label-free electrochemical immunosensor for the detection of the ovarian cancer biomarker CA125 based on CuCo-ONSs@AuNPs nanocomposites, J. Pharm. Biomed. Anal. 243 (2024) 116080. https://doi.org/10.1016/j.jpba.2024.116080.
[71] A.B. Beiranvand, F. Tadayon, H. Bagheri, Direct detection of lymphoma cancer cells based on impedimetric immunosensors, RSC Adv. 15 (2025) 9884–9890. https://doi.org/10.1039/D4RA07801B.
[72] F. Geng, Y. Li, Q. Wu, C. Ding, An efficient electrochemical biosensor based on double-conductive hydrogel as antifouling interface for ultrasensitive analysis of biomarkers in complex serum medium, Sens. Actuators B Chem. 422 (2025) 136625. https://doi.org/10.1016/j.snb.2024.136625.
[73] T. Lin, Y. Shen, Fabricating electrochemical aptasensors for detecting aflatoxin B1 via layer-by-layer self-assembly, J. Electroanal. Chem. 870 (2020) 114247. https://doi.org/10.1016/j.jelechem.2020.114247.
[74] C. Erkmen, G.A. Tiğ, B. Uslu, First label-free impedimetric aptasensor based on Au NPs/TiO2 NPs for the determination of leptin, Sens. Actuators B Chem. 358 (2022) 131420. https://doi.org/10.1016/j.snb.2022.131420.
[75] Y. Jiang, D. Sun, Z. Liang, L. Chen, Y. Zhang, Z. Chen, Label-free and competitive aptamer cytosensor based on layer-by-layer assembly of DNA-platinum nanoparticles for ultrasensitive determination of tumor cells, Sens. Actuators B Chem. 262 (2018) 35–43. https://doi.org/10.1016/j.snb.2018.01.194.
[76] O. Hanpanich, A. Lomae, A. Maruyama, T. Palaga, O. Chailapakul, N. Ngamrojanavanich, Label-free detection of HPV mRNA with an artificial chaperone-enhanced MNAzyme (ACEzyme)-based electrochemical sensor, Biosens. Bioelectron. 221 (2023) 114352. https://doi.org/10.1016/j.bios.2022.114352.
[77] Y. Vojgani, S. Ranjbar, N. Naseri, A. Dolati, Z. Madjd, J. Kiani, S. Saeedi, M. Karimi, Quantitative measurement of CA 15-3 cancer biomarker using an electrochemical aptasensor based on the electrodeposition of Au thin film on cauliflower-like rGO-MoS2 nanocomposite, Microchim. Acta 190 (2023) 406. https://doi.org/10.1007/s00604-023-05989-4.
[78] R. Khan, A.S. Deshpande, G. Proteasa, S. Andreescu, Aptamer-based electrochemical biosensor with S protein binding affinity for COVID-19 detection: Integrating computational design with experimental validation of S protein binding affinity, Sens. Actuators B Chem. 399 (2024) 134775. https://doi.org/10.1016/j.snb.2023.134775.
[79] L.-L. Long, W.-X. Hu, X. Wang, R. Yuan, Y.-Q. Chai, Antibody-Protein-Aptamer Electrochemical Biosensor based on Highly Efficient Proximity-Induced DNA Hybridization on Tetrahedral DNA Nanostructure for Sensitive Detection of Insulin-like Growth Factor-1, Anal. Chem. 96 (2024) 3837–3843. https://doi.org/10.1021/acs.analchem.3c05035.
[80] L.A. Wasiewska, F.G. Diaz, H. Shao, C.M. Burgess, G. Duffy, A. O'Riordan, Highly sensitive electrochemical sensor for the detection of Shiga toxin-producing E. coli (STEC) using interdigitated micro-electrodes selectively modified with a chitosan-gold nanocomposite, Electrochimica Acta 426 (2022) 140748. https://doi.org/10.1016/j.electacta.2022.140748.

[81] S. Kasturi, Y. Eom, S.R. Torati, C. Kim, Highly sensitive electrochemical biosensor based on naturally reduced rGO/Au nanocomposite for the detection of miRNA-122 biomarker, J. Ind. Eng. Chem. 93 (2021) 186–195. https://doi.org/10.1016/j.jiec.2020.09.022.

[82] T.S. Martins, J.L. Bott-Neto, O.N. Oliveira, S.A.S. Machado, A sandwich-type electrochemical immunosensor based on Au-rGO composite for CA15-3 tumor marker detection, Microchim. Acta 189 (2022) 38. https://doi.org/10.1007/s00604-021-05145-w.

[83] P. Samadi Pakchin, H. Ghanbari, R. Saber, Y. Omidi, Electrochemical immunosensor based on chitosan-gold nanoparticle/carbon nanotube as a platform and lactate oxidase as a label for detection of CA125 oncomarker, Biosens. Bioelectron. 122 (2018) 68–74. https://doi.org/10.1016/j.bios.2018.09.016.

[84] Y. Yan, Z. Qiao, X. Hai, W. Song, S. Bi, Versatile electrochemical biosensor based on bi-enzyme cascade biocatalysis spatially regulated by DNA architecture, Biosens. Bioelectron. 174 (2021) 112827. https://doi.org/10.1016/j.bios.2020.112827.

[85] L. Durai, S. Badhulika, Highly selective trace level detection of DNA damage biomarker using iron-based MAX compound modified screen-printed carbon electrode using differential pulse voltammetry, Sens. Actuators Rep. 3 (2021) 100057. https://doi.org/10.1016/j.snr.2021.100057.

Captions

Figure 1: Schematic representation of a LbL assembly-based biosensor architecture. a) Bare electrochemical transducer, exemplified by a screen-printed electrode (SPE), b) modification of the working electrode (WE) surface with a nanomaterial, c) immobilisation of a bioreceptor and d) detection of the target analyte.

Figure 2. Application of LbL-EC techniques in the assembly and characterisation of immunosensors. Schematic illustration of a layer-by-layer (LbL) immunosensor assembly monitored by cyclic voltammetry (CV) and electrochemical impedance spectroscopy (EIS). a) SPE bare WE. b) WE modification with biochar, a sustainable carbon nanomaterial that acts both as an electrochemical enhancer (increasing Ip, reducing ΔE and Rct) and as an anchoring platform for bioreceptors. c) Covalent immobilisation of the secondary antibody (AbII) via EDC/NHS-mediated amide coupling. d) Immobilisation of the primary antibody (AbI). e) Target recognition, exemplified here by viral analyte binding. Adapted from Cancelliere et al. (2022)[38].

Table 1. Overview of commonly employed techniques in the characterisation of multilayer sensor architectures.

Technique	Information provided	Advantages	Limitations
SEM / TEM	Morphology, defect sites, nanoscale structural detail	High-resolution structural imaging	Static snapshots; require vacuum; unsuitable for soft or hydrated architectures
STM / AFM	Surface topology, molecular packing density	Atomic- to nanoscale resolution	Surface-limited; no in-operando monitoring; extremely sensitive to environmental noise
CV / EIS (LbL-EC)	Charge transfer kinetics, layer homogeneity, interfacial dynamics	Real-time, in-operando, functional characterisation	Complex interpretation; spatial averaging masks nanoscale heterogeneity
Hybrid approaches	Integrated structural and functional readouts	Multiscale, comprehensive insight	Increased experimental complexity; requires multimodal expertise

Table 2. Representative examples of LbL-EC applied to EB development over the last three years. The table highlights the diversity of targets (proteins, nucleic acids, toxins, metabolites, pathogens), the biorecognition strategies employed (antibodies, aptamers, enzymes, DNA probes), and the integration of nanostructured materials for enhanced performance. Reported limits of detection (LOD) and complementary non-electrochemical characterisation techniques are included to illustrate how LbL-EC provides functional insights that bridge structural analysis and device optimisation.

Target	Type of biosensor	Layers materials	LbL-EC technique	Not LbL-EC technique	LOD	Reference
IL-6	Immuno.	BP-PAMI, Abs	CV EIS	AFM TEM Zeta Potential XPS Raman XRD	1 pg/ml	[49]
OLA	Immuno.	GO, AgNPs, PEI, AuNPs, Abs	CV EIS DPV	SEM TEM UV-vis XRD	4.8 pg/ml	[53]
CYFRA21-1	Immuno.	Si_3N_4/MoS_2–MWCNTs, Abs, MMSNs@AuNPs	CV EIS DPV	SEM TEM XRD XPS FTIR	2.0 fg/ml	[54]
VEGF	Immuno.	rGO, Abs	CV SWV	SEM Raman XPS	0.1 pg/ml	[55]
SARS-CoV-2 S protein	Immuno.	Cu2O NCs, Prot A, Abs	CV, EIS		0.04 fg/ml	[56]
IL-1β	Immuno.	Au–Ag–MoS_2-rGO, peptide	CV EIS SWV	XRD XPS FE-SEM	2.4 pM	[57]
TNF- α	Immuno.	MoS_2 nf, Abs	CV EIS	XRD SEM TEM AFM Raman	0.202 pg/ml	[58]
Ochratoxin A	Immuno.	MBA, Abs	CV EIS	AFM	0.19 ng/ml	[59]

α-synuclein protein	**Immuno.**	**AuNPs, Abs**	**EIS SWV DPV CA**	**DLS AFM FE-SEM EDX**	**4 ng/ml**	[60]
β-Amyloid1-42	**Immuno.**	**PtCOCuNPs/rGO, Abs**	**CV EIS CA**	**TEM XPS EDX SEM**	**3.5 fg/ml**	[61]
CEA, CA125, CA153, CA199	**Immuno.**	**PBNCs, cryogel, Abs**	**CV EIS**	**SEM AFM**	**CEA: 0.79 pg/mL, CA125: 0.37 mU/mL, CA153: 0.49 mU/mL, CA199: 0.48 mU/mL**	[62]
Quinalphos	**Immuno.**	**PVA/Gelatin–AuNPs nanofiber, nanobody**	**EIS**	**FTIR SEM AFM**	**50.74 pg/ml**	[63]
PSA	**Immuno.**	**Fe-Cu LDH, rGO, Abs**	**CV EIS**	**FE-SEM EDX XRD FTIR**	**63.24 fg/ml**	[64]
Ochratoxin A	**Immuno.**	**AuNPs, Abs**	**EIS**	**EDS SEM AFM Raman**	**0.15ng/ml**	[65]
α-synuclein	**Immuno.**	**SWCNTs AuNPs, Abs**	**CV EIS SWV**	**SEM**	**4.1 pg/ml**	[66]
CA125	**Immuno.**	**CuCo-ONSs@AuNPs, Abs**	**CV EIS DPV**	**SEM TEM XRD XPS**	**3.9×10^{-8} U/mL**	[67]
Lymphoma cancer cells	**Immuno.**	**AuNPs@DTSP, BA, Ab, BSA**	**EIS**	**TEM FT-IR**	**62 cell/ml**	[68]
CEA	**Apta.**	**KMPPH, aptamer**	**EIS CV DPV**	**XRD FT-IR TEM SEM**	**0.41 pg/ml**	[69]

AFB1	**Apta.**	**Aptamer, GNs, PSCOOH NPs, PDDA**	**CV EIS**	**FE-SEM TEM**	**0.002 ng/ml**	[70]
Leptin	**Apta.**	**TiO2NPs, AuNPs, Aptamer**	**CV EIS**	**SEM**	**0.312 pg/ml**	[71]
HepG2 cells	**Apta.**	**AuNPs, aptamer, PtNPs**	**CV EIS DPV**	**DLS SEM TEM**	**15 cell/ml**	[72]
HPV mRNA	**Apta.**	**AuNPs, Hairpin, PLL-*g*-Dex**	**CV EIS DPV**	**SEM**	**0.88pM**	[73]
CA15-3	**Apta.**	**AuTF, rGO-MoS_2**	**CV EIS**	**XRD FE-SEM EDS**	**0.3 U/ml**	[74]
viral S protein	**Apta.**	**AuNPs, aptamer**	**CV DPV**	**SEM**	**91.1pM**	[75]
Growth Factor-1	**Apta-Immuno.**	**TDN, Abs**	**CV EIS SWV**	**PAGE AFM TEM UV-vis**	**0.47 fM**	[76]
***stx1* gene**	**DNA**	**AuNPs, Chitosan, DNA-probe**	**CV EIS SWV**	**FM SEM EDX**	**100 aM**	[77]
miRNA-21	**DNA**	**rGO, AuNPs, DNA probe**	**CV EIS DPV**	**XRD FTIR EDS XPS**	**1.73 pM**	[78]
CA15-3	**Enz.**	**rGO-AuNPs, Abs, HRP-Abs**	**CV EIS SWV**	**SEM EDS**	**0.08 fg/ml**	[79]
CA125	**Enz.**	**CS-AuNP/MWCNT/G, Abs, AuNPs-Lox-Abs**	**CV EISCA**	**XRD, DLS, SEM,TEM, UV-Vis**	**0.002 U/mL**	[80]
cancerous exosomes and thrombin	**Enz.**	**GOx/HRP DFs, aptamer**	**CV EIS DPV**	**SEM TEM DLS**	**Exosomes: $1.02 \cdot 10^3$ particles/µL Thrombin: 12.77 fM,**	[81]

8-OHdG	**Other**	**Fe_3AlC_2 nanoflakes**	**CV DPV CC**	**XRD SEM**	**50 pM**	[82]

Achronyms:

Immunosensor (Immuno), Aptamer (Apta.), Enzyme (Enz.) Cyclic Voltammetry (CV), Electrochemical impedance spectroscopy (EIS), differential pulsed voltammetry (DPV), Square wave voltammetry (SWV), Chronoamperometry (CA), Chronocoulometry (CC), Scanning Electron Microscopy (SEM), Transmission Electron Microscopy (TEM), Atomic Force Microscopy (AFM), X-ray Photoelectron Spectroscopy (XPS), X-ray Diffraction (XRD), Fourier Transform Infrared Spectroscopy (FT-IR), Field Emission Scanning Electron Microscopy (FE-SEM), Energy Dispersive X-ray Spectroscopy (EDX), Energy Dispersive Spectroscopy (EDS), Dynamic Light Scattering (DLS), Polyacrylamide Gel Electrophoresis (PAGE), Fluorescence Microscopy (FM), black phosphorene-polyallylamine (BP-PAMI), Antibodies (Abs), Graphene oxide (GO), Silver Nanoparticles (AgNPs), Gold Nanoparticles (AuNPs), Polyethyleneimine (PEI), Multi-Walled Carbon Nanotubes (MWCNTs), magnetic mesoporous silica nanoparticles@gold nanoparticles (MMSNs@AuNPs), reduced Graphene Oxide (rGO), nanocubes (NCs), Protein A (Prot A), nanoflower (nf), Mercaptobenzoic acid (MBA), Prussian Blue Nano Cubes (PBNCs), Polyvinyl alcohol (PVA), layered double hydroxide (LDH), nanogold-functionalized copper-cobalt oxide nanosheets (CuCo-ONSs@AuNPs), 3,3′-dithiodipropionic acid (DTSP), Boronic Acid (BA), Bovine Serum Albumin (BSA), K-MXene-PEDOT:PSS-PNIPAM hydrogels (KMPPH), N-doped graphene nanosheets (GNs), Polystyrene (PS), Poly(diallyl dimethylammonium chloride) solution (PDDA), Poly($_L$-lysine)-*graft*-dextran (PLL-*g*-Dex), gold thin film (AuTF), tetrahedral DNA nanostructure (TDN), Horseradish Peroxidase (HRP), Chitosan-gold nanoparticle (CS-AuNP), lactate oxidase (LOx), DNA flowers (DFs), Interleukin-6 (IL-6), Olaquindox (OLA), vascular endothelial growth factor (VEGF), interleukin-1beta (IL-1β), Tumor Necrosis Factor-α (TNF-α), carcinoembryonic antigen (CEA), carbohydrate antigen 125 (CA125), carbohydrate antigen 153 (CA153), carbohydrate antigen 199 (CA199), 8-hydroxy-2′-deoxyguanosine (8OHdG)

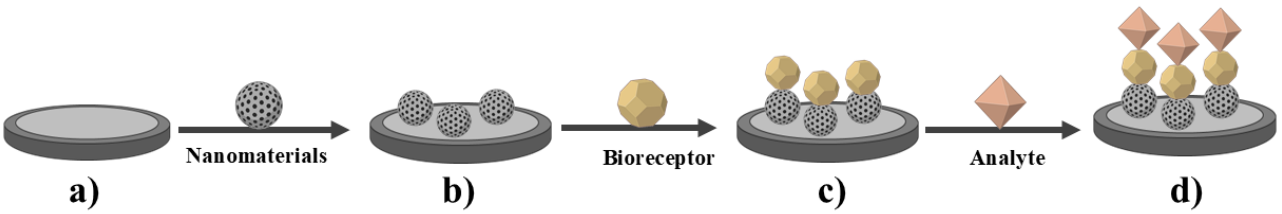

Figure 1.

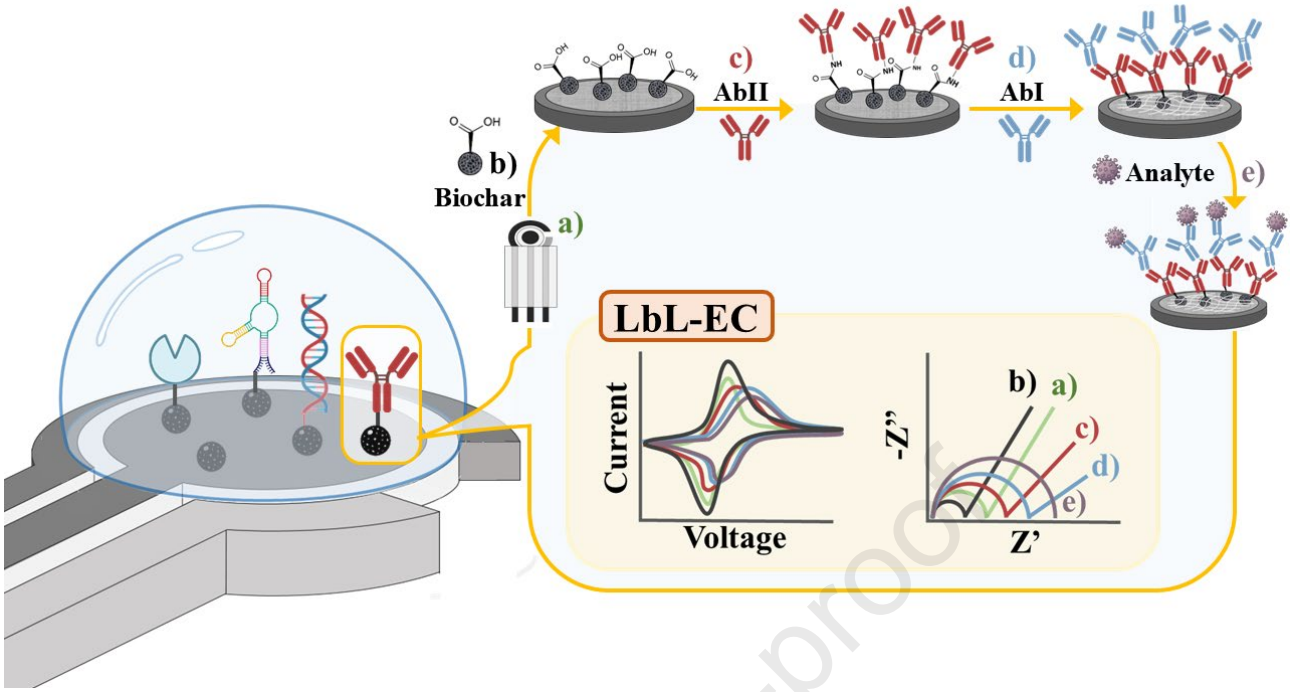

Figure 2.

Highlights

- Layer-by-layer (LbL) modified electrode for (Bio)sensing.
- Theoretical principles for electrochemical layer-by-layer characterization (LbL-EC) multi-layer architectures.
- LbL-EC strategy in multi-layer-based (Bio)sensors characterization, fabrication and optimization.
- Interpretation of Biosensing mechanism using LbL-EC.
- Future perspectives for LbL-EC in electrochemical (bio)sensors.

References and Recommended Reading

Papers of special interest, published within the last two years, have been highlighted as:

(*) of special interest

(**) of outstanding interest

[10] R. Boukherroub, S. Szunerits, The Future of Nanotechnology-Driven Electrochemical and Electrical Point-of-Care Devices and Diagnostic Tests, Annu. Rev. Anal. Chem. 17 (2024) 173–195. https://doi.org/10.1146/annurev-anchem-061622-012029.

(**) *The identification of key cutting-edge technology and discussion of nanomaterial-driven solutions that are likely to define the future of electrochemical diagnostics and personalized healthcare make this work of outstanding interest.*

[11] H. Duan, S. Peng, S. He, S. Tang, K. Goda, C.H. Wang, M. Li, Wearable Electrochemical Biosensors for Advanced Healthcare Monitoring, Adv. Sci. 12 (2025) 2411433. https://doi.org/10.1002/advs.202411433.

(*) *Reviews state-of-the-art wearable electrochemical biosensors, with emphasis on flexible architectures and real-time physiological monitoring.*

[12] D. Wachholz Junior, P.B. Deroco, B.M. Hryniewicz, L.T. Kubota, Strategies for Electrochemical Point-of-Care Biosensors, Annu. Rev. Anal. Chem. 18 (2025) 307–333. https://doi.org/10.1146/annurev-anchem-071124-103739

(*) *Reviews recent strategies for electrochemical point-of-care biosensors, highlighting advances in fabrication, biorecognition, and multiplexed detection toward integrated, low-cost diagnostic systems.*

[14] M. Barawi, C.A. Mesa, L. Collado, I.J. Villar-García, F. Oropeza, V.A. De La Peña O'Shea, M. García-Tecedor, Latest advances in *in situ* and *operando* X-ray-based techniques for the characterisation of photoelectrocatalytic systems, J. Mater. Chem. A 12 (2024) 23125–23146. https://doi.org/10.1039/D4TA03068K.

(*) *Provides a comprehensive and critical overview of in situ and operando X-ray-based techniques (XPS, XAS, XRD) for photoelectrocatalytic systems, offering technical guidance and conceptual advances that are transforming the real-time characterization of solar-driven electrochemical interfaces*.

[32] H. Zhang, Z. Sun, K. Sun, Q. Liu, W. Chu, L. Fu, D. Dai, Z. Liang, C.-T. Lin, Electrochemical Impedance Spectroscopy-Based Biosensors for Label-Free Detection of Pathogens, Biosensors 15 (2025) 443. https://doi.org/10.3390/bios15070443.

(*) Provides a comprehensive and technically detailed review of electrochemical impedance spectroscopy for label-free pathogen detection, highlighting advances in nanomaterial interfaces and point-of-care integration.

[40] B.L. Huffman, A.R.C. Bredar, J.L. Dempsey, Origins of non-ideal behaviour in voltammetric analysis of redox-active monolayers, Nat. Rev. Chem. 8 (2024) 628–643. https://doi.org/10.1038/s41570-024-00629-8.

(**) *Provides a comprehensive and mechanistic framework for understanding the origins of non-ideal voltammetric behaviour in redox-active monolayers, integrating theory and experiment to redefine how molecular disorder is interpreted at electrochemical interfaces.*

[52] R. Cancelliere, M. Molinara, A. Licheri, A. Maffucci, L. Micheli, Artificial intelligence-assisted electrochemical sensors for qualitative and semi-quantitative multiplexed analyses, Digit. Discov. 4 (2025) 338–342. https://doi.org/10.1039/D4DD00318G.

(**) *Introduces a novel AI-driven approach for multiplexed voltammetric analysis, using Gramian Angular Field transformations and convolutional neural networks to resolve overlapping electrochemical signals with high accuracy, marking a transformative step toward intelligent electrochemical sensing.*

[69] F. Geng, Y. Li, Q. Wu, C. Ding, An efficient electrochemical biosensor based on double-conductive hydrogel as antifouling interface for ultrasensitive analysis of biomarkers in complex serum medium, Sens. Actuators B Chem. 422 (2025) 136625. https://doi.org/10.1016/j.snb.2024.136625.

(*) Demostrates an innovative electrochemical antifouling biosensor based on a double-conductive hydrogel integrating MXene and PEDOT:PSS , enabling unltrasensitive detection of carcinoembryonic antigen in complex serum matrices with a detection limit down to the pg mL-1 range. This approach significantly improves analytical performance and reliability in real biological samples.

Conflict of Interest and Authorship Conformation Form

- All authors have participated in (a) conception and design, or analysis and interpretation of the data; (b) drafting the article or revising it critically for important intellectual content; and (c) approval of the final version.

- This manuscript has not been submitted to, nor is under review at, another journal or other publishing venue.

- The authors have no affiliation with any organization with a direct or indirect financial interest in the subject matter discussed in the manuscript

Declaration of interests

☐ The authors declare that they have no known competing financial interests or personal relationships that could have appeared to influence the work reported in this paper.

☒ The authors declare the following financial interests/personal relationships which may be considered as potential competing interests:

Micheli Laura reports financial support was provided by University of Rome Tor Vergata Department of Chemical Sciences and Technologies. If there are other authors, they declare that they have no known competing financial interests or personal relationships that could have appeared to influence the work reported in this paper.